

The Extended Cycle of Solar Activity and the Sun's 22-Year Magnetic Cycle

E.W. Cliver

Received: 13 May 2014 / Accepted: 14 August 2014 / Published online: 18 September 2014
© Springer Science+Business Media Dordrecht 2014

Abstract The Sun has two characteristic migrations of surface features—the equatorward movement of sunspots and the poleward movement of high-latitude prominences. The first of these migrations is a defining aspect of the 11-yr Schwabe cycle and the second is a tracer of the process that culminates in solar polarity reversal, signaling the onset of the 22-yr magnetic cycle on the Sun. Zonal flows (torsional oscillations of the Sun's differential rotation) have been identified for both of these migrations. Helioseismology observations of these zonal flows provide support for the extended (>11 -yr cycle) of solar activity and offer promise of a long-term precursor for predicting the amplitude of the Schwabe cycle. We review the growth of observational evidence for the extended and 22-yr magnetic cycles and discuss: (1) the significance of latitude $\sim 50^\circ$ on the Sun; (2) the “over-extended” cycle; and (3) the outlook for solar cycle 25.

Keywords Extended solar cycle · 22-Yr magnetic cycle · Schwabe cycle · Sunspots · Polar crown filaments

1 Introduction

“Solar periodicity is a most complex phenomenon. The more it is studied, the less it seems to be understood.” Thus wrote Agnes Mary Clerke, the authoritative chronicler of 19th century astronomy, in 1903. In the intervening 100 plus years, our knowledge of the 11-yr solar cycle has increased dramatically (e.g., Hathaway 2010; Charbonneau 2010), but the understanding remains a challenge. For example, the 79 predictions for the peak smoothed sunspot number for cycle 24 reviewed by Pesnell (2012) range from 42 to 185, with the most probable value being nearer the lower end of that range (the current observed peak is ~ 75 at the time of this writing). “Prediction . . .,” as Clerke wrote, “remains at fault.” Here we review the evolution of knowledge on the extended 18–22 year cycle of solar activity (Wilson et al. 1988) and the Sun's 22-yr magnetic cycle (Hale and Nicholson 1925; Babcock 1961). We

E.W. Cliver (✉)
National Solar Observatory, Sunspot, NM, USA
e-mail: ecliver@nso.edu

focus on the two characteristic migrations of surface features on the Sun: the equatorward movement of sunspot formation and the poleward movement of high-latitude prominence formation.

Sections 2 and 3 cover historical observations of sunspot and prominence migration and the discovery of the 22-yr magnetic cycle on the Sun, respectively. In Sect. 4, we review recent work on zonal flows of the Sun's differential rotation in relation to the extended and 22-yr cycles. Certain aspects of the extended activity cycle and the 22-yr magnetic cycle are discussed further in Sect. 5.

2 Cyclic Migrations of Sunspots and Prominences

2.1 Movement of Sunspot Formation Toward the Equator

Carrington (1858) discovered the latitude variation of sunspot formation over the 11-yr Schwabe (1844) cycle. He wrote,

...throughout the two years preceding the minimum of frequency in February 1856, the spots were confined to an equatorial belt, and in no instance passed the limits of 20° of latitude N. or S.; and that shortly after this epoch, whether connected with it or not, this equatorial series appears to have become extinct, and in seeming contradiction to the precept, *Natura non agit per saltum* [Nature makes no leaps], two new belts of disturbance abruptly commenced, the limits of which in both hemispheres, may be roughly set at between 20° and 40° , with exceptions in favor of the old equatorial region. The tendency at the present time appears to be contraction of the parallels.

In his book *Spots on the Sun*, Carrington (1863) wrote that the two fresh belts of sunspots that formed at high latitudes in the northern and southern hemisphere following the 1856 minimum “have in subsequent years shown a tendency to coalesce and ultimately contract as before to extinction. Whether this is what appears at each period of increase and decrease of frequency of the Spots must be left to observers who may follow me to show. At present it is only probable that such is the case, and another contribution made to facts on the broad scale which will ultimately elucidate the origin of this phenomenon and instruct us on the question, ‘What is a Sun?’ ”

The pattern deduced by Carrington was codified by Spörer (1880) and illustrated by Maunder (1904) in the original butterfly diagram (Fig. 1) for cycles 12 and 13. Figure 2 gives portraits of Edward Maunder and his wife Annie Russell Maunder who assisted him in the production of this iconic figure. Many years later, Annie Maunder (1940) described the circumstances surrounding its creation, “We made this diagram in a week of evenings, one dictating and the other ruling these little lines. We had to do it in a hurry because we wanted to get it before the [Royal Astronomical] Society at the same meeting as the other sunspot observers, whose views we knew to be heretical. As it turned out, this paper, especially the diagram—wiped Father Cortis’ and Prof. Lockyer’s papers clean off the slate, and fully established the manner of procedure of the sunspot 11-year cycle.”

2.2 Movement of Low-Latitude Prominences Toward the Equator and High-Latitude Prominences Toward the Poles

Two other husband and wife teams (Evershed and Evershed 1917; d’Azambuja and d’Azambuja 1948) helped to establish the cyclic migrations of prominences during the

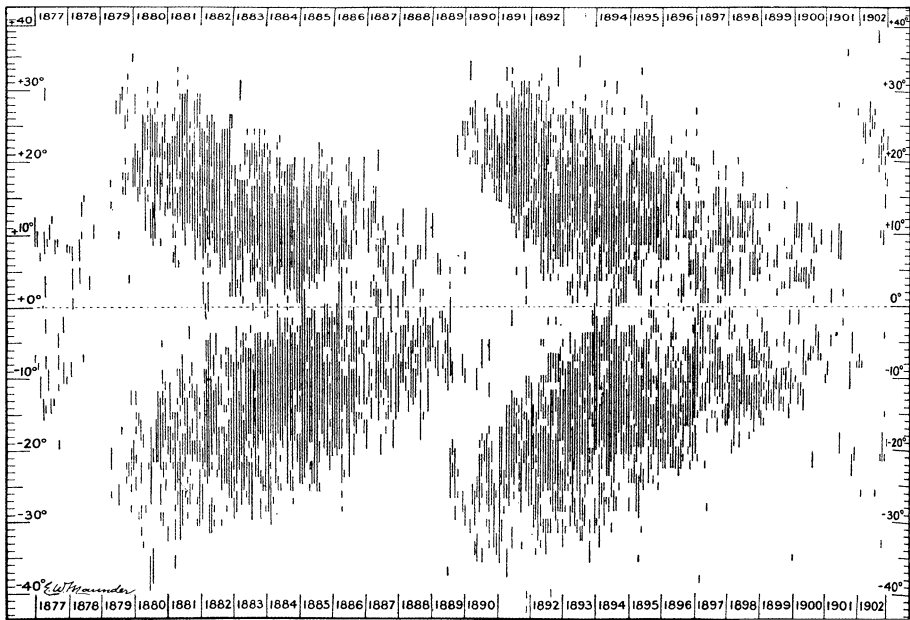


Fig. 1 The Maunder butterfly diagram showing the latitude distribution of sunspots for Schwabe cycles 12 and 13 (from Maunder 1904)

Fig. 2 Edward Walter Maunder (1851–1928) and Annie Russell Maunder (1868–1947). Photo from Kinder (2008), date unknown (With permission of the British Astronomical Association)



solar cycle—the equatorward movement of low-latitude prominence formation in concert with sunspots and the poleward movement of high-latitude prominence formation. An undated photograph circa 1915 of John and Mary Acworth Evershed (fifth and 6th from left in the second row) with the staff at Kodaikanal Observatory is given in Fig. 3. The Italian school of astronomers that included Respighi, Secchi, and Tacchini were the first to note that prominences appeared near the poles only at solar maximum (Lockyer 1931; Waldmeier 1973). The Eversheds credit Riccò with discovering the general laws of prominence distribution in latitude over the solar cycle and Lockyer and Lockyer (1902) with confirming them. A stylized diagram of the migrations of high- and low-latitude prominences from Riccò (1892) is shown in Fig. 4. Importantly, this figure shows oppositely directed migrations of high-latitude and low-latitude prominences starting from mid-latitudes near solar minimum. The depicted poleward migration of low-latitude prominences toward

Fig. 3 John Evershed (1864–1956) and Mary Acworth Evershed (1867–1949), fifth and sixth from right in the second row, with the staff of the Kodaikanal Observatory circa 1915 (With permission of the Observatory Science Centre, Herstmonceux/Terence Evershed)



Fig. 4 Stylized diagram of the migrations of prominences over the solar cycle (from Riccò 1892). It captures the equatorward and poleward migrations of prominences that begin near solar minimum. The maximum to minimum phase depicted here is incorrect (see text)

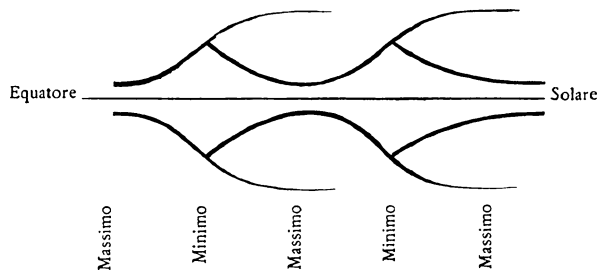
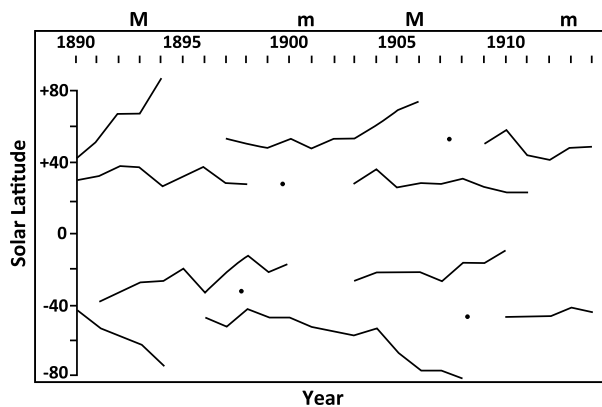


Fig. 5 Migration of prominences in latitude during cycles 13, 14, and the onset of cycle 15 (from Evershed and Evershed 1917), based on observations from Kenley and Kodaikanal. The *black dots* refer to “a few sporadic zones which do not seem to play a part in the history of [the] main zones”. Times of solar minima (*m*) and maxima (*M*) are indicated



mid-latitudes following solar maximum, however, is erroneous. Figure 5, taken from Evershed and Evershed (1917) and covering the interval from 1890–1914 shows that, following the disappearance in each solar cycle of the polar prominences, a new high-latitude branch forms at about 50° latitude in both hemispheres where it resides during the decay of the cycle to begin migrating poleward near solar minimum. This poleward migration was referred to by the Eversheds as a “dash to the pole” and in current usage has come to be called “the

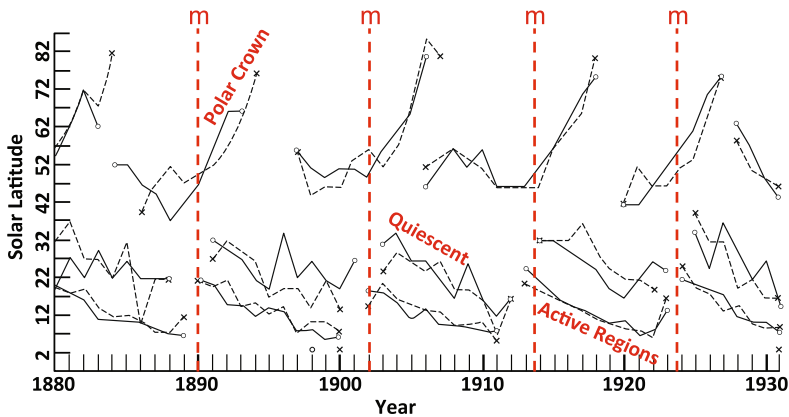


Fig. 6 Prominence migrations during cycles 12–15 (adapted from Bocchino 1933). Data for 1880–1911 are from Arcetri and for 1911–1930 are from various observatories including Catania, Madrid, and Zürich. Tracks are shown in each hemisphere for the polar crown filaments (*top*), the quiescent filaments that lay 10–15° poleward of the sunspots (*middle*), and active region filaments (*bottom*; based on sunspot observations). Solar minima (*m*) are marked by *dashed red lines*

rush to the poles” (e.g., Ananthkrishnan 1954; Altrock 1997, 2014). A separate low-latitude branch forms after solar minimum and moves equatorward.

An expanded plot of this behavior for the years 1880–1930 (adapted from Bocchino 1933) is given in Fig. 6. Here it can be seen that the time-averaged migratory behavior of the prominences (or filaments when viewed on the disk) is as systematic as that of the sunspots. For each solar cycle, three distinct branches of prominence activity can be seen or inferred in each hemisphere: (a) a high-latitude branch that moves poleward following solar minimum; (b) a lower-latitude branch which mimics the progression of sunspots toward the equator but is offset from the sunspot curve by $\sim 10\text{--}15^\circ$ toward the poles; and (c) a branch that overlays the sunspot migration. The three tracks in Fig. 6 correspond, respectively, to the three classes of prominences defined by Waldmeier (1973): long-lived “polar crown” prominences/filaments that form at latitudes above 45° following sunspot maximum, long-lived quiescent prominences that have their maximum frequency of occurrence about $10\text{--}15^\circ$ poleward of the sunspot zone, and active region prominences (which originally included such phenomena as sprays and post-eruption loop systems). The cyclic migrations of the high- and low-latitude quiescent filament branches in Fig. 6 have been supported/extended in subsequent studies by d’Azambuja and d’Azambuja (1948), Ananthkrishnan and Nayar (1954), Ananthkrishnan (1954), Li et al. (2008), and Li (2010). There are differences in details among the various works that can be attributed to different latitude/time averaging intervals and data sets. Recent developments in the automatic recognition of solar filaments (e.g., Bernasconi et al. 2005; Labrosse et al. 2010; Schuh et al. 2014) promise to standardize the results of such work.

The three tracks in Fig. 6 do not indicate motion of individual prominences but rather, just as is the case for sunspots, the migration of the locations of prominence formation (i.e., filament channels; Martin 1998; Mackay et al. 2014). Even the longest-lived prominences, those in the polar crown, have maximum individual lifetimes of only about eight months (Smith and Smith 1963)—short in comparison with their migration times to the pole.

3 Magnetic Polarity Reversals

3.1 Sunspots and the Hale-Nicholson Polarity Rule

In 1908 George Ellery Hale used the Zeeman (1897) effect to make his epochal discovery of strong magnetic fields in sunspots (Hale 1908). Hale et al. (1919) reported that before the minimum in 1912 preceding cycle 15, “the magnetic polarity of unipolar spots and of the preceding members of bipolar spots was positive [north] in the southern and negative [south] in the northern hemispheres of the Sun. Since the minimum these signs have reversed.” At the sunspot number minimum in 1923, the sunspot polarities for new solar cycle 16 in each hemisphere reverted to the polarities of cycle 14. This enabled Hale and Nicholson (1925) to formulate the law of sunspot polarities: “The sun-spots of a new 11½-year cycle, which appear in high latitudes after a minimum of solar activity, are of opposite magnetic polarity in the northern and southern hemispheres. As the cycle progresses the mean latitude of the spots in each hemisphere steadily decreases, but their polarity remains unchanged. The high-latitude spots of the next 11½-year cycle, which begin to develop more than a year before the low-latitude spots of the preceding cycle have ceased to appear, are of opposite magnetic polarity.” Anticipating the subsequent polarity reversal at the end of cycle 16, Hale and Nicholson noted that while the periodicity in the number of spots was 11½ years, the full sunspot period, which they called the “magnetic sun-spot period”, was 23 years. Today, this magnetic cycle is generally referred to as the 22-yr, or Hale, cycle based on a nominal 11-yr Schwabe cycle.

3.2 Reversal of the Sun’s Polar Field

The father and son team of Harold and Horace Babcock, shown in Fig. 7, used the newly-developed solar magnetograph (Babcock 1953) of the Hale Solar Laboratory to detect a general (now called polar) magnetic field of the Sun of ~ 1 G based on magnetograms taken from the interval August 1952 to October 1954 that spanned the April 1954 solar minimum preceding cycle 19 (Babcock and Babcock 1955). Hale (1913) had been the first to attempt to look for such a field but, using the instrumentation available at the time, deduced a field of ~ 50 G. The solar polar field (generally confined to latitudes $> 55^\circ$) that the Babcocks detected was positive in the north and negative in the south (opposite to that of Earth). Babcock and Babcock noted that the polar fields during this period showed no signs of reversal that might have been expected to accompany the change in the hemispheric polarity of sunspots over the 11-yr minimum. From the d’Azambuja’s description of the poleward migration of the polar crown filaments, Babcock and Babcock presciently inferred that the general field of the Sun would reverse polarity at the maximum of cycle 19—out of phase with the polarity reversal for the sunspot curve. Babcock (1959) subsequently observed this reversal of the dipolar field of the Sun, with the field at the north heliographic pole changing in mid-1957 and the field in the south reversing in November 1958. The separation in time between the polar field reversal in the two hemispheres is now recognized to be a common feature of the reversal of the large-scale polar field (Svalgaard and Kamide 2013). As expected (Babcock 1961), the polar fields appeared to reverse, at least in the northern hemisphere, near the maximum of cycle 20 (Howard 1972) but they were weak relative to the magnetograph noise, making it difficult to determine the exact timing. Here was a different, more fundamental, 22-yr magnetic cycle, extending from (approximately) sunspot maximum to maximum over two ~ 11 year intervals, rather than from minimum to minimum.

Fig. 7 Harold Delos Babcock (1882–1968) and Horace Welcome Babcock (1912–2003) (HDB image courtesy of the Archives, California Institute of Technology; HWB image courtesy of the Observatories of the Carnegie Institution for Science Collection at the Huntington Library, San Marino, California)



3.3 Reversal of the Flanking Magnetic Fields of the Polar Crown Filaments

There is evidence that the classical picture of the migration of the polar crown filaments in Fig. 6 is overly-simplistic. Topka et al. (1982) and Makarov and Sivaraman (1989a, 1989b) showed that in a given hemisphere for certain cycles there can be multiple rushes to the poles of bands of filaments rather than a single poleward rush leading to polarity reversal. Topka et al. start the migration of the secondary and tertiary polar crown branches, in such sequences, at latitudes above $\sim 20^\circ$, similar to the poleward moving ripples in B_r reported by Ulrich and Tran (2013). Waldmeier (1973) had earlier noted the existence of a secondary zone of high-latitude northern-hemisphere prominences that reached the pole during cycle 20. No such occurrence had been observed for cycles 12 through 18, but Waldmeier allowed that a secondary rush of this type might have escaped notice in earlier cycles. Makarov and Sivaraman (1989a) reported even more complex behavior for cycle 20 in the north—a three-fold polarity reversal (– to +, + to –, and – to +), consistent with Topka et al. (1982). Moreover, they deduced similar three-fold reversals in a single hemisphere for cycles 12, 14, 16, and 19. Subsequently, Dermendjiev et al. (1994) reported a secondary polar crown in the southern hemisphere in cycle 22. Presumably, such multiple poleward migrations are related to the quasi-periodic ~ 1 – 3 year fluctuations seen in the sunspot record (Krivova and Solanki 2002) and in the stronger surges of magnetic flux to high latitudes seen in butterfly diagrams of photospheric magnetic fields (Fig. 8, taken from Ulrich and Tran 2013).

Instead of the usual method of obtaining a mean or average location for the various types of filaments (in which an arbitrary latitude—usually in the range from 40 – 60° (e.g., Bretz and Billings 1959; Waldmeier 1973; Li et al. 2008; Kong et al. 2014)—is used to separate the polar crown filaments from low-latitude filaments), Hansen and Hansen (1975) presented plots of all filaments observed on the Sun during several consecutive Carrington rotations. The composite plot they constructed by tracing outlines of filaments in the *Cartes Synoptiques* for the July–December 1967 interval is shown in Fig. 9 where it can be seen that the polar crown filament in each hemisphere at this time lies at a latitude of $\sim 60^\circ$. Equatorward of the polar crown filaments lies a band of filaments that extend poleward to the east; these filaments are flanked on their north and south sides by opposite magnetic polarities to those in the polar crown and lie about $\sim 15^\circ$ from the polar crown filaments with a relatively well-defined gap in between.

McIntosh (1992) constructed the plot in Fig. 10 by taking the latitudes of the two most poleward filaments for each solar rotation, in both hemispheres. This shows clearly, at least for cycles 21 and 22, the rush to the poles of the polar crown filament beginning near solar

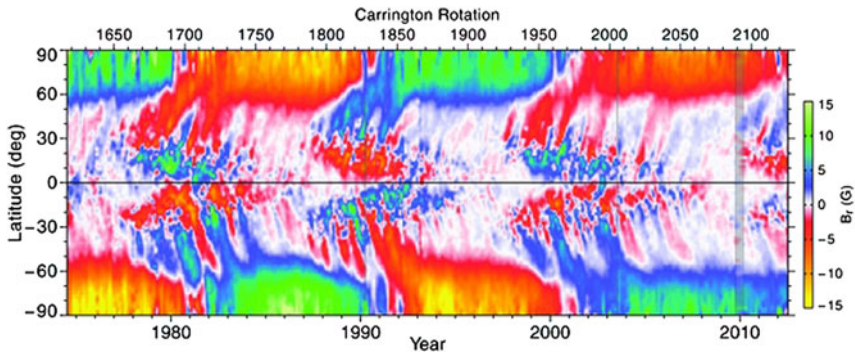


Fig. 8 Latitudinal variation of the radial component of the photospheric magnetic field from mid-1974 to mid-2012 (from Ulrich and Tran 2013) (©AAS. Reproduced with permission)

Fig. 9 Superposed tracings of all filaments in the *Cartes Synoptiques* for July–December 1967 (from Hansen and Hansen 1975) (With kind permission from Springer Science and Business Media)

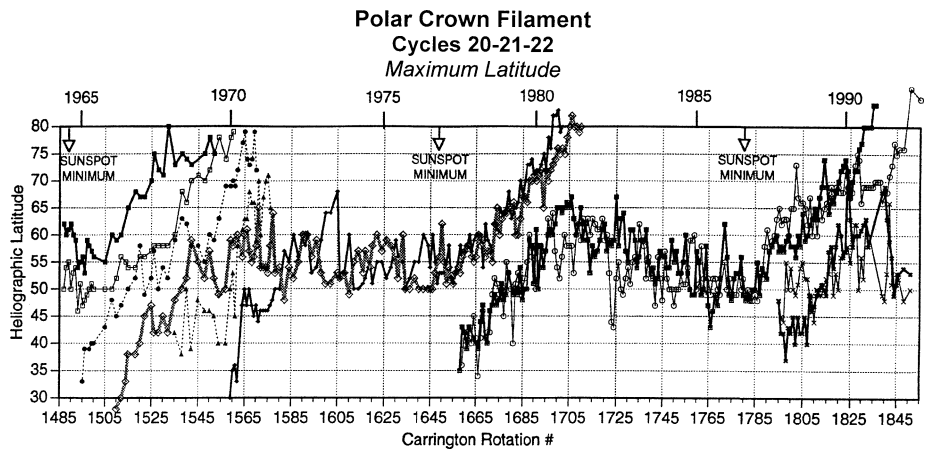
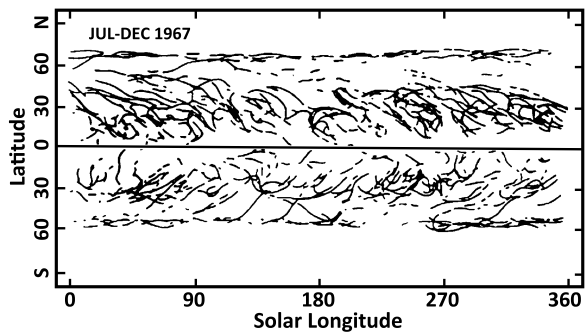
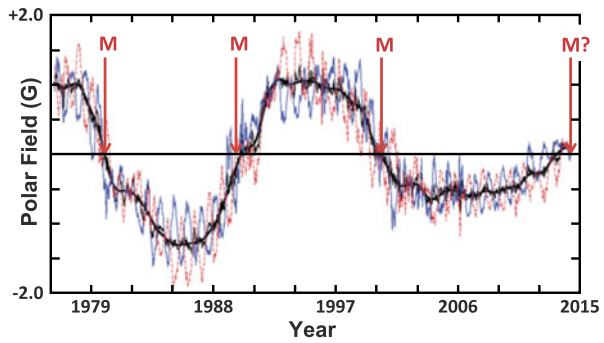


Fig. 10 Maximum latitudes of filaments in the true and replacement polar crowns for both hemispheres for cycles 20–22 (from Webb 1997; McIntosh 1992). For cycle 21, the true polar crown begins the rush to the poles in both hemispheres from $\sim 55^\circ$ in 1976. The replacement polar crown (true polar crown for cycle 22) begins moving poleward shortly thereafter from $\sim 40^\circ$ latitude. High-latitude filament behavior was more complex in cycle 20 (see text)

Fig. 11 Solar polar field strength from Wilcox Solar Observatory for 1976 to mid-2014 for the North (solid blue) and South (dashed red; negated) hemispheres



minimum and the corresponding poleward progression of the replacement polar crown with opposite flanking polarities for the new magnetic cycle. As noted above, the march to the poles of the polar crown for cycle 20 and its replacement by the polar crown for cycle 21 was less stately. The onset of poleward movement of both types of filaments (true and replacement polar crown) in Fig. 10 occurs near sunspot minimum. The disappearance of the polar crown filaments in each hemisphere occurs near the time of the reversal of the polar fields (e.g., Waldmeier 1960) and sunspot maximum (Fig. 11). Here the reversal of the polar fields refers to the passage of the polar field strength through zero. As can be seen in Fig. 11, it takes several years for the field strength of the new field polarity to reach maximum. Ulrich and Tran (2013) note that the initial broad surges of poleward moving flux in the northern hemisphere in Fig. 8 are closely associated with the polarity reversals near 1980, 1990, and 2000. Reversal is more complicated in the south although in each case, it follows that in the north within ~ 1 year. The replacement (new cycle) polar crown reaches its apex (at latitudes of $\sim 60\text{--}70^\circ$) near polarity reversal and then, as the new polar crown, drifts equatorward to $\sim 50\text{--}55^\circ$ where it resides before beginning its own rush to the poles near solar minimum (Fig. 10). From a study of quiescent prominences at the end of cycle 20 (1973–1976) that employed the Hanle (1924) effect, Leroy (1978) showed that the magnetic polarities flanking the polar crown filaments were opposite to those deduced by Rust (1967) from magnetograph observations during 1964–1965 at the end of cycle 19.

4 Cyclic Zonal Flows

The notion of an extended solar cycle of 12–14 (rather than ~ 11) years originated in the 19th century but it was the discovery of torsional oscillations of the Sun's surface rotation in Mt. Wilson Doppler data by Howard and LaBonte (1980) and LaBonte and Howard (1982) (see also Snodgrass 1985, 1992; Ulrich 2001; Howe et al. 2011) that brought the concept to wide attention. The torsional oscillations reported by Howard and LaBonte (1980) provided evidence for an even longer extended cycle. They moved from pole to equator, starting near solar minimum, over a ~ 22 -year interval. The torsional oscillations consist of alternating bands of faster and slower velocities, relative to the nominal differential rotation. The latitudinal derivative of the torsional oscillations, corresponding to maximal velocity shear, bisects the wings of the sunspot butterfly diagram in each hemisphere. As noted by LaBonte and Howard (1982), the torsional oscillations were the first large-scale velocity fields that were closely related to the solar cycle in space and time. The torsional oscillations are currently also referred to as migrating zonal (parallel to the equator) flow bands or simply zonal

flows (Howe 2009). Similar, but slightly different, migrating patterns in the differential rotation have also been detected by tracking surface magnetic features (e.g., Komm et al. 1993). In this case the strong magnetic field regions coincide with bands of slower-than-average zonal flow.

Interest in the torsional oscillations or zonal flow bands was reinvigorated about twenty years after their 1980 discovery when they were detected in helioseismology studies (Schou 1999; Howe et al. 2000b; Toomre et al. 2000) based on inversion of rotational splittings of solar oscillation frequencies (e.g., Thompson et al. 1996; Schou et al. 1998; Howe 2009) observed by the *Michelson Doppler Imager* (MDI; Scherrer et al. 1995) on the *Solar and Heliospheric Observatory* (SOHO; Domingo et al. 1995) and by the *Global Oscillation Network Group* (GONG; Harvey et al. 1996). Subsequent studies revealed that the zonal flows persisted deep into the convection zone (Howe et al. 2000a; Antia and Basu 2000; Vorontsov et al. 2002). Moreover, the zonal flows detected by this method exhibited a high-latitude poleward-moving branch (Antia and Basu 2001; Vorontsov et al. 2002) in addition to the equatorward-moving branch discovered by Howard and LaBonte.

Generally, the torsional oscillations are viewed as a secondary or side effect of the magnetic activity cycle on the Sun's differential rotation (Gilman 1992), in part because the maximum amplitude of the flow is only $\sim 5 \text{ m s}^{-1}$ against a solar mean rotation rate at the equator of $\sim 2000 \text{ m s}^{-1}$ (and a more comparable mean velocity change across 1° of latitude of $\sim 15 \text{ m s}^{-1}$ in the sunspot zone). Proposed mechanisms to account for the torsional oscillations (see Howe 2009, for a review) include: Lorentz force feedback from the magnetic cycle (Schüssler 1981; Yoshimura 1981), thermal feedback (Spruit 2003), magnetic quenching of (small-scale) turbulent angular momentum transport (Küker et al. 1999; Pipin 1999), or a combination of these effects (Rempel 2006). Recently, Beaudoin et al. (2013) attributed the zonal flows to modulation of angular-momentum transport by large-scale meridional flow.

4.1 The Extended Cycle of Solar Activity and the Equatorward-Propagating Branch of the Zonal Flows

There are several lines of evidence that the solar activity cycle is longer than the nominal 11-yr sunspot cycle. The first indication came from the sunspots themselves. Figure 12, taken from Clerke (1903) shows Spörer's observations of the mean latitude of sunspots during solar cycles 10 and 11. Quoting from Clerke, "spot production at minima [occurs in] two widely separated zones in each hemisphere . . . the start of a new series [of sunspots] in high latitudes [anticipates] the termination of the old. . . [Figure 12] illustrates the nature of the progression. The overlapping of the curves at minimum brings before us the remarkable circumstance that, as a consequence of successive disturbances breaking out before those antecedent to them have expired, the full duration of each [cycle] is, not eleven but twelve to fourteen years." Harvey (1992) compiled and re-analyzed reports of the first and last magnetic bipoles, including ephemeral regions (Harvey and Martin 1973; Harvey et al. 1975; Martin and Harvey 1979) and Ca^+ plage regions, for solar cycles 14–22 (Table 1), assigning regions to cycles on the basis of latitude, magnetic polarity, and "an understanding of the characteristics of the magnetic configuration of active regions as a function of latitude and time." The entries for more recent cycles in the table, which are based on higher resolution data, indicate a latitude range of $\sim 30\text{--}60^\circ$ for the first bipoles in a cycle and extended cycle durations of $\sim 14\text{--}16$ years.

Observations of the 5303 Å coronal green line (e.g., Waldmeier 1960; Leroy and Noens 1983; Altrock 1997, 2014) reveal enhanced emission that appears at latitudes $\sim 70^\circ$ near the

Fig. 12 Overlapping mean latitude curves of sunspots (*bold lines*) for cycles 10 and 11 as determined by Spörer (adapted from Young 1897; reproduced in Clerke 1903)

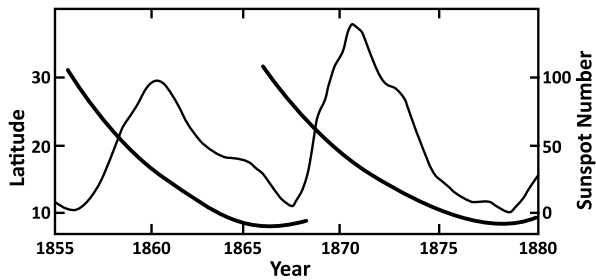


Table 1 First and last magnetic bipoles observed from cycles 14–22 and comparison of the resulting extended cycle with the corresponding minimum-to-minimum cycle (from Harvey 1992)

Cycle N	First region			Last region			Cycle duration (yrs)	
	Lat.	Year	Δt_N	Δt_{N+1}	Year	Lat.	Extended	Min-min
14	S21	1900.61	-1.1	+1.9	1915.45	N01	15.8	11.9
15	N20	1911.96	-1.6	+1.5	1925.13	N08	13.2	10.0
16	N34	1921.75	-1.8	+1.9	1935.51	N04	13.8	10.0
17	N48	1932.04	-1.6	+2.0	1946.19	N01	14.2	10.6
18	S30	1942.25	-2.0	+2.2	1956.53	N01	14.3	10.6
19	N42	1953.12	-1.2	+2.2	1967.12	S01	14.0	10.6
20	N46	1962.79	-2.1	+2.0	1978.45	S01	15.7	11.6
21	N61	1973.04	-3.5	+1.7	1988.48	S02	15.4	10.3
22	N32	1983.31	-3.5					

11-yr cycle maximum and migrates equatorward to apparently join and move in concert with the progression of sunspot formation to lower latitudes as can be seen in the composite in Fig. 13 for cycles 18–20 (Leroy and Noens 1983). The continuation of this behavior in cycles 21 through 23 is shown in Fig. 14 from Altrock et al. (2008). Extended cycle lengths deduced from green line measurements are ~17–18 years. As noted above, the surface torsional oscillations reported by Howard and LaBonte (1980) moved from pole to equator over a 22-year interval.

Wilson et al. (1988) compiled the lines of evidence available at that time to argue for an extended solar cycle of 18–22 years (Fig. 15). Since the overlap between 11-yr sunspot cycles had been known since the 19th century and the coronal green line has been routinely monitored since 1939 (Rybanský et al. 2005), the torsional oscillations along with the ephemeral regions of Harvey and Martin were the key new pieces of evidence that drew attention to an extended cycle, in this case up to twice as long as the Schwabe cycle.

Even before the Wilson et al. (1988) paper, however, the 22-yr duration of the torsional oscillations was being questioned. Snodgrass (1985) reanalyzed the Mt. Wilson Doppler data and concluded that the torsional oscillation began during ~1973.5–1974.5, roughly three years after the polar field reversal (Makarov and Sivaraman 1989a) and closer to latitude 45° than 90° in both hemispheres, although it appeared to end at ~10° near the maximum of the following cycle rather than at the equator near minimum.

The equatorward zonal flow discovered via helioseismology in cycle 23 began at ~45° in 2003 (Fig. 16; Howe et al. 2013), about three years after polarity reversal (Fig. 11). This delay from polarity reversal and mid-latitude onset were consistent with that inferred from

Fig. 13 Superposed epoch plot of the standard deviation of 5303 Å emission at each latitude recorded at Pic du Midi from 1944–1974 showing high-latitude (rush to the poles) and low-latitude (sunspot-related) branches of coronal emission (from Leroy and Noens 1983) (Reproduced with permission ©ESO)

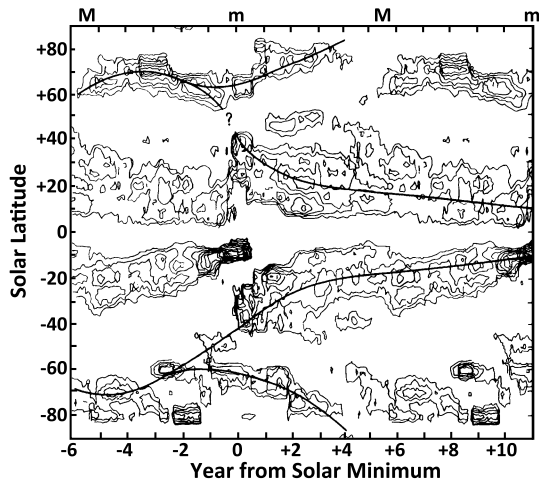


Fig. 14 Annual northern- plus southern-hemisphere averages of the number of coronal activity local maxima from 1973 through 2006 (from Altrock et al. 2008)

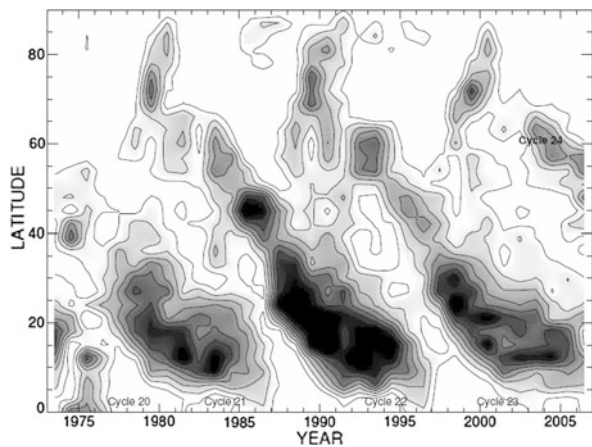
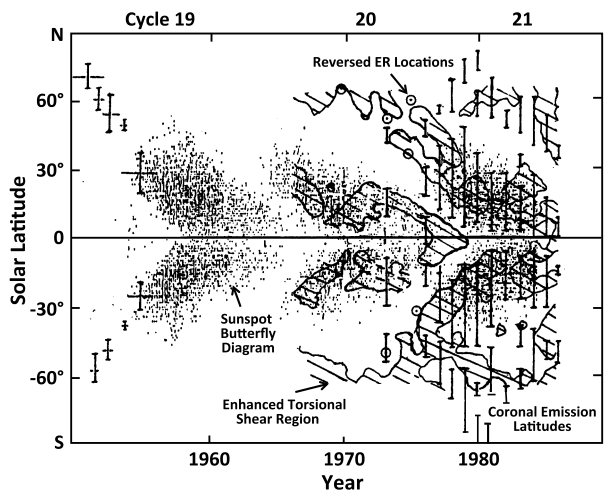


Fig. 15 The extended solar cycle for cycles 19–21 showing the time and latitudinal extension of the sunspot cycle inferred from reversed polarity ephemeral active regions (*circles with dots*), coronal green line emission (*vertical lines*), and the torsional oscillations (contoured hatching) (adapted from Wilson et al. 1988) (Adapted by permission from Macmillan Publishers Ltd: Nature)



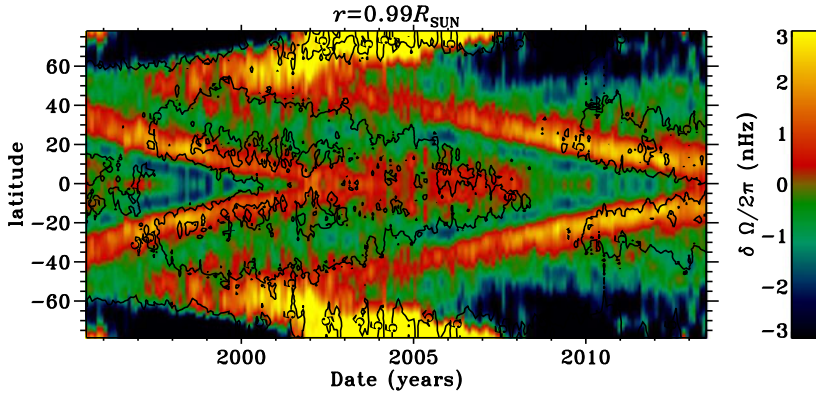


Fig. 16 Zonal flow pattern, symmetrized about the equator, at $0.99 R_{\odot}$ for mid-1995 to mid-2013 based on GONG, MDI, and Heliospheric Magnetic Imager (HMI; Schou et al. 2012) observations showing the poleward- and equatorward-migrating branches (adapted and updated from Howe et al. 2013) (©AAS. Reproduced with permission)

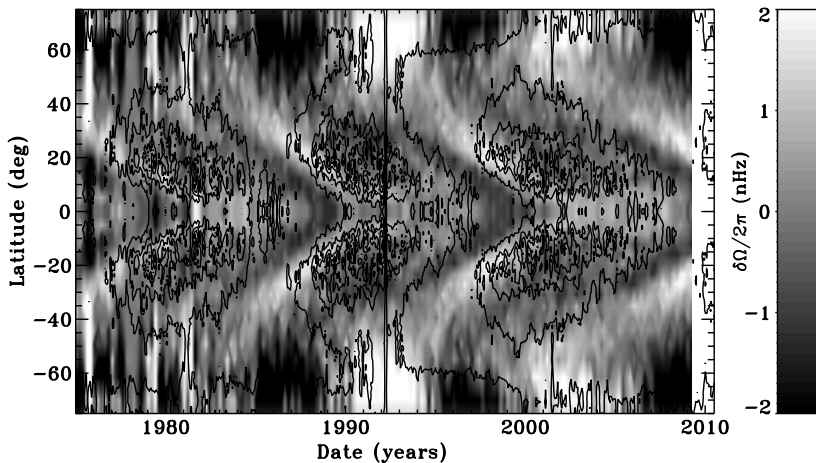


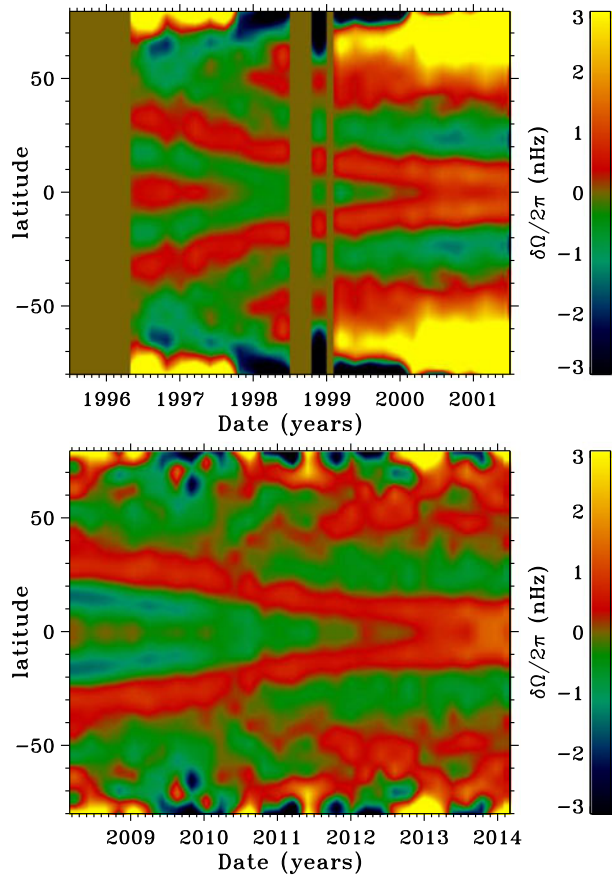
Fig. 17 Zonal flows at the Sun's surface deduced from Doppler measurements at Mt. Wilson 1975–2009; black contours give the unsigned magnetic field strength (adapted from Howe et al. 2011). Both data sets are symmetrized about the equator

spectroscopic observations by Snodgrass (1985) for the onset of the zonal flows in cycle 20. Figure 16 also shows that the low-latitude zonal flow for cycles 22 and 23 ended within about one year of the 11-yr minima in 1996 and 2008, in agreement with the finding of Howard and LaBonte (1980) for cycle 20. Thus the zonal flow observations yield a pattern for the equatorward flows that is more limited in latitude and time than that reported by Howard and LaBonte (1980). This can also be seen in Fig. 17 from Howe et al. (2011) that shows surface Doppler measurements from Mt. Wilson for cycles 21–23.

4.2 The Poleward-Propagating Zonal Flow and the 22-Yr Cycle of Solar Activity

Just as the rush to the poles of the high-latitude prominences was discovered later and is less well-known than the equatorward propagation of sunspots during the 11-yr cycle, so too the

Fig. 18 Rotation rate residuals at $0.99 R_{\odot}$ from MDI/HMI for comparable intervals in cycles 23 (top) and 24 (bottom). Note the relative weakness of the polar flows in cycle 24 (2009–present) relative to cycle 23 (1996–2008) (adapted and updated from Howe et al. 2013) (©AAS. Reproduced with permission)



poleward-moving branch of the torsional oscillations (Fig. 16) was discovered later than the equatorward moving branch and as a result has been less well-studied. Howard and LaBonte (1980) did not detect a poleward-propagating branch of the torsional oscillations, although Livingston and Duvall (1979) had reported a “spin-up” of the high-latitude rotation rate near the solar maximum of solar cycle 20. Subsequently, Snodgrass (1985) reported fast zonal flows at high latitudes at or near the maxima of both cycles 20 and 21. Discovery of the high-latitude poleward-moving branch by seismological methods (Antia and Basu 2001) was also delayed slightly relative to that of the low-latitude equatorward moving branch. The high-latitude branch was found to penetrate to the tachocline (Vorontsov et al. 2002; Basu and Antia 2003).

The polar zonal flow is intimately connected (either as a tracer or a driver) to the reversal of the Sun’s polar fields, and thus the 22-yr magnetic cycle, in space and time. The rush to the poles of the polar crown filaments in cycles 20–22 lags the preceding 11-yr minima by intervals ranging from ~ 5 –20 solar rotations (Fig. 10). For comparison the onset of the poleward moving branch of the zonal flows in cycles 23 and 24 lags the preceding minima by ~ 10 and ~ 20 rotations, respectively (Figs. 16 and 18). From approximately 2002 through 2004 the polar flow is a prominent feature above 60° (Fig. 16). The mean polar field reached its maximum field strength in 2004 (Fig. 11). The subsequent decay of the polar

around latitude 50° , to which they hold with lessened frequency throughout sunspot minimum, until with the rising activity of a new cycle, they rise to maximum frequency and ‘rush to the pole’ [Fig. 6].”

The diverging migrations of low- and high-latitude filaments beginning near solar minimum were qualitatively illustrated by Riccò in 1892, and documented in the first half of the 20th century by Evershed and Evershed (1917), Bocchino (1933), and d’Azambuja and d’Azambuja (1948). Nevertheless, the notion of a latitudinal divide in solar activity at $\sim 50^\circ$, between the upper limit of the extended cycle and the solar minimum residence of the polar crown filaments has not taken hold. The transition at $\sim 50^\circ$ between the equatorward- and poleward migrations of zonal flows (Antia and Basu 2001; Vorontsov et al. 2002) brings renewed attention to this latitude (Fig. 19).

5.2 The Over-extended Cycle

The premise of the extended cycle is that the equatorward migration of sunspots during a given solar cycle can be extended to higher latitudes and earlier times by considering forms of solar activity that can be detected prior to sunspots. One such type of activity is the torsional oscillation. The Wilson et al. (1988) proposal of an 18–22 year cycle was based in large part on Howard and LaBonte’s (1980) finding that the torsional oscillation extended from $\sim 90^\circ$ to $\sim 0^\circ$ over 22 years, beginning at solar minimum. However, helioseismology analysis of the zonal flows (Fig. 16) indicate a starting latitude of the equatorward-moving branch of $\sim 45^\circ$ and a corresponding reduction in length of the proposed extended cycle.

Wilson et al. also included coronal green line emission as evidence for a high-latitude ($>70^\circ$) origin for the extended cycle. The green line emission exhibits both a high-latitude branch associated with the rush to the poles and an equatorward-moving branch associated with sunspot formation. Figure 13 shows how the two may be conflated. In this figure, at about the same time the high-latitude emission in the northern hemisphere is moving equatorward to $\sim 60^\circ$, the green line emission associated with the extended cycle is making its appearance near 40° . One is inclined to connect the dots—thereby erroneously linking the two fundamentally different migrations of solar activity—at the time/latitude where Leroy and Noens (1983) cautiously inserted a question mark. The behavior of the high-latitude branch has been recently modeled by Robbrecht et al. (2010) using data from the Extreme-ultraviolet Imaging Telescope (Delaboudinière et al. 1995). They associate the high-latitude EUV emission with the boundary of the polar coronal hole (Wang et al. 1997; Benevolenskaya et al. 2001). In simple terms, the sequential equatorward, then poleward, motion of the band of high-latitude coronal emission (and the underlying polar crown filament, Fig. 10) following polarity reversal is viewed as a reflection of the waxing and waning of the polar coronal hole as the polar field first strengthens during the decline of the cycle and then begins to weaken near minimum (Fig. 11) in concert with the rush to the poles. In a latitude vs. time plot, the migration track of the polar crown filaments (and associated high-latitude green line emission) makes a U-turn (Fig. 19). Comparison of Figs. 10 and 11 shows that the stationary residence of the new polar crown filament at $\sim 50\text{--}60^\circ$ preceding the 1986 solar minimum corresponds to the broad maximum in polar field strength. Altrock (2014) has presented recent green-line evidence for the extended cycle beginning at 65° in ~ 2003 during cycle 24. However, like Robbrecht et al. (2010), Tappin and Altrock (2013) and Altrock (2014) link the high-latitude emission to streamers overlying polar crown filaments which do not migrate below $\sim 50^\circ$ to become part of the extended cycle.

Recently, Petrie et al. (2014) have re-visited the analysis of Robbrecht et al. (2010) and concluded that “The question of whether the extended cycle connects more to the main

cycle or the march to the poles phenomena in green line variance remains open. The evidence more strongly indicates connection with the main cycle [as seen in their Fig. 7, our Fig. 16], and this would match the patterns of the interior torsional oscillations and photospheric ephemeral bipoles." Physically linking the contiguous high-latitude and low-latitude branches of the green line emission in Figs. 13 and 14 has the appeal of Occam's razor. The preponderance of evidence, however, supports the picture of Benevolenskaya et al. (2001) and Robbrecht et al. (2010). For example, in the contour diagram in Fig. 14 of 5303 Å peaks, consider the enhancements between $\sim 67\text{--}77^\circ$ centered on ~ 1979.5 and ~ 1989.5 that appear to be the highest latitude components of an extended cycle. Comparison with the McIn-tosh plot of polar crown filaments in Fig. 10 indicates that in 1979 and 1989 the polar crown filaments were located between $\sim 65\text{--}75^\circ$, while undergoing their rush to the poles during cycles 21 and 22, respectively. Inspection of the magnetic butterfly diagram in Fig. 8 reveals strong poleward surges of trailing polarity flux with leading edges between $\sim 60\text{--}65^\circ$ in both hemispheres at these times. The relative locations of green line enhancements, polar crown filaments, and magnetic flux surges in these two cases are consistent with the picture that the green line emission overlies the polar crown filaments and results from the encroachment of trailing polarity magnetic flux on the opposite polarity flux of the polar coronal hole. Both Benevolenskaya et al. (2001) and Robbrecht et al. (2010) stress the role of trailing polarity flux in creating the enhanced high-latitude green line emission but it seems clear that poleward "counter-surges" of leading polarity flux (Ulrich and Tran 2013) will also play a role, particularly later in the cycle, for the new polar crown filament which has opposite flanking magnetic polarities to that of its predecessor (Fig. 19). Such counter-surges may contribute to the concentrations of 5303 Å peaks at $\sim 55\text{--}65^\circ$ centered at ~ 1983.5 , ~ 1993 , and ~ 2004 in Fig. 14. Finally, the interior torsional oscillations to which Petrie et al. (2014) refer appear to originate at $\sim 45^\circ$ latitude (Fig. 16) rather than the higher latitudes of these green line features while the new cycle ephemeral regions exhibit broad latitudinal scatter which straddles the polar crown magnetic inversion line (see Fig. 5 in Harvey 1994). Nonetheless, we agree with Petrie et al. (2014) that further study of the latitudinal limit of the green line manifestation of the extended cycle is in order.

To summarize, there is an extended cycle, as was known since the 19th century (Fig. 12) from sunspot data. An 18–22 year ($\sim 70^\circ\text{--}0^\circ$) extended cycle is not supported by the data although a 13–16 year cycle (Table 1), assuming a nominal 11-yr Schwabe cycle, that extends poleward to the $\sim 50^\circ$ delineator between the equatorward motion of ephemeral regions/sunspots and the poleward movement of polar crown filaments is well-established, and is supported by observations of green line emission (Figs. 13 and 14) and zonal flows (Figs. 16 and 17).

5.3 The Poleward-Propagating Branch of Zonal Flow During Cycle 24 and the Amplitude of Cycle 25

The rush to the poles phenomenon first observed in solar prominences and subsequently in the coronal green-line emission and the zonal flows is intimately connected with polarity reversal and the ensuing development of the polar fields. The polar field strength at solar minimum is thought to be the most reliable precursor for predicting the peak sunspot number of the following cycle (e.g., Schatten et al. 1978; Svalgaard et al. 2005). The onset of the rush to the poles phenomenon precedes the peak of the cycle whose amplitude it is linked to by ~ 15 years (e.g., 1997 rush to poles onset in cycle 23 (Fig. 14) and ~ 2014 cycle 24 maximum), making it a potential long-term predictor of solar cycle amplitude. More realistically, if mid-term (3–5 years after onset) development of the high-latitude zonal flow

has predictive value, the schematic in Fig. 19 indicates a lead time of ~ 10 years. Thus (echoing Komm et al. 2014), it will be of great interest to see if the stunted development of the poleward-propagating zonal flows (Fig. 18) and green line emission in cycle 24 (Altrock 2014), relative to cycle 23, translate into a further reduction in the cycle-to-cycle polar field strength at the next minimum and a prediction that cycle 25 will be weaker than cycle 24.

Acknowledgements I thank Andr  Balogh, Hugh Hudson, Krist f Petrovay, and Rudolf von Steiger for organizing a timely and stimulating workshop. I am grateful to: Dick Altrock, Rainer Arlt, Sara Martin, Alexei Pevtsov, and Leif Svalgaard for helpful comments/discussions, Tom Bogdan for providing the text of A. Maunder's letter, and Rachel Howe for providing updated/modified versions of Figs. 16, 17, and 18.

References

- R.C. Altrock, An 'extended solar cycle' as observed in FeXIV. *Sol. Phys.* **170**, 411–423 (1997)
- R.C. Altrock, Forecasting the maxima of solar cycle 24 with coronal Fe XIV emission. *Sol. Phys.* **289**, 623–629 (2014)
- R. Altrock, R. Howe, R. Ulrich, Solar torsional oscillations and their relationship to coronal activity, in *Sub-surface and Atmospheric Influences on Solar Activity*, ed. by R. Howe, R.W. Komm, K.S. Balasubramanian, G.J.D. Petrie. ASP Conference Series, vol. 383 (2008), pp. 335–342
- R. Ananthkrishnan, Prominence activity (1905–1952). *Proc. Indian Acad. Sci.* **40**, 72–90 (1954)
- R. Ananthkrishnan, P.M. Nayar, Discussions of the results of observations of solar prominences made at Kodaikanal from 1905–1950. Bulletin No. 137 of Kodaikanal Observatory (1954)
- H.M. Antia, S. Basu, Temporal variations of the rotation rate in the solar interior. *Astrophys. J.* **541**, 442–448 (2000)
- H.M. Antia, S. Basu, Temporal variations of the solar rotation rate at high latitudes. *Astrophys. J. Lett.* **559**, L67–L70 (2001)
- H.W. Babcock, The solar magnetograph. *Astrophys. J.* **118**, 387–396 (1953)
- H.D. Babcock, The Sun's polar magnetic field. *Astrophys. J.* **130**, 364–365 (1959)
- H.W. Babcock, The topology of the Sun's magnetic field and the 22-year cycle. *Astrophys. J.* **133**, 572–587 (1961)
- H.W. Babcock, H.D. Babcock, The Sun's magnetic field, 1952–1954. *Astrophys. J.* **121**, 349–366 (1955)
- S. Basu, H.M. Antia, Changes in solar dynamics from 1995 to 2002. *Astrophys. J.* **585**, 553–565 (2003)
- P. Beaudoin, P. Charbonneau, E. Racine, P.K. Smolarkiewicz, Torsional oscillations in a global solar dynamo. *Sol. Phys.* **282**, 335–360 (2013)
- E.E. Benevolenskaya, A.G. Kosovichev, J.R. Lemen, P.H. Scherrer, G.L. Slater, Detection of high-latitude waves of solar coronal activity in extreme-ultraviolet data from the Solar and Heliospheric Observatory EUV Imaging Telescope. *Astrophys. J. Lett.* **554**, L107–L110 (2001)
- P.N. Bernasconi, D.M. Rust, D. Hakim, Advanced automated solar filament detection and characterization code: description, performance, and results. *Sol. Phys.* **228**, 97–117 (2005)
- G. Bocchino, Migrazione delle protuberanze durante il ciclo undecennale dell'attivit  solare. *Oss. Mem. Oss. Astrofis. Arcetri* **51**, 5–47 (1933)
- M.C. Bretz, D.E. Billings, Analysis of emission corona 1942–1955 from Climax spectrograms. *Astrophys. J.* **129**, 134–145 (1959)
- R.C. Carrington, On the distribution of the solar spots in latitudes since the beginning of the year 1854, with a map. *Mon. Not. R. Astron. Soc.* **19**, 1–3 (1858)
- R.C. Carrington, *Observations of the Spots on the Sun from November 9, 1853 to March 24, 1861* (Williams and Norgate, London, 1863), p. 17
- P. Charbonneau, Dynamo models of the solar cycle. *Living Rev. Sol. Phys.* **7**, 3 (2010)
- A.M. Clerke, *Problems in Astrophysics* (Black, London, 1903), pp. 150–152
- L. d'Azambuja, M. d'Azambuja, A comprehensive study of solar prominences and their evolution from spectroheliograms obtained at the observatory and from synoptic maps of the chromosphere published at the observatory. *Ann. Obs. Meudon* **6**(Fasc. VII), 1–278 (1948)
- J.-P. Delaboudini re, G.E. Artzner, J. Brunaud, A.H. Gabriel, J.F. Hochedez, F. Millier, X.Y. Song, B. Au et al., EIT: extreme-ultraviolet imaging telescope for the SOHO mission. *Sol. Phys.* **162**, 291–312 (1995)
- V.N. Dermendjiev, K.Y. Stavrev, V. Rušin, M. Rybansky, Secondary polar zone of prominence activity revealed from Lomnický Štít observations. *Astron. Astrophys.* **281**, 241–244 (1994)
- V. Domingo, B. Fleck, A.I. Poland, The SOHO mission: an overview. *Sol. Phys.* **162**, 1–37 (1995)
- J. Evershed, M.A. Evershed, Results of prominence observations. *Mem. Kodaikanal Obs.* **1**, 55–126 (1917)

- P.A. Gilman, What can we learn about solar cycle mechanisms from observed velocity fields? in *The Solar Cycle*, ed. by K.L. Harvey. ASP Conference Series, vol. 27 (ASP, San Francisco, 1992), pp. 241–255
- G.E. Hale, On the probable existence of a magnetic field in sun-spots. *Astrophys. J.* **28**, 315–343 (1908)
- G.E. Hale, Preliminary results of an attempt to detect the general magnetic field of the Sun. *Astrophys. J.* **38**, 27–98 (1913)
- G.E. Hale, S.B. Nicholson, The law of sun-spot polarity. *Astrophys. J.* **62**, 270–300 (1925)
- G.E. Hale, F. Ellerman, S.B. Nicholson, A.H. Joy, The magnetic polarity of sun-spots. *Astrophys. J.* **49**, 153–178 (1919)
- W. Hanle, Über magnetische Beeinflussung der Polarisation der Resonanzfluoreszenz. *Z. Phys.* **30**, 93–105 (1924)
- R. Hansen, S. Hansen, Global distribution of filaments during solar cycle no. 20. *Sol. Phys.* **44**, 225–230 (1975)
- K.L. Harvey, The cyclic behavior of solar activity, in *The Solar Cycle*, ed. by K.L. Harvey. ASP Conference Series, vol. 27 (ASP, San Francisco, 1992), pp. 335–367
- K.L. Harvey, The solar magnetic cycle, in *Solar Surface Magnetism*, ed. by R.J. Rutten, C.J. Schrijver (Kluwer, Dordrecht, 1994), pp. 347–363
- K.L. Harvey, S.F. Martin, Ephemeral active regions. *Sol. Phys.* **32**, 389–402 (1973)
- K.L. Harvey, J.W. Harvey, S.F. Martin, Ephemeral active regions in 1970 and 1973. *Sol. Phys.* **40**, 87–102 (1975)
- J.W. Harvey, F. Hill, R. Hubbard, J.R. Kennedy, J.W. Leibacher, J.A. Pintar, P.A. Gilman, R.W. Noyes et al., The global oscillation network group (GONG) project. *Science* **272**, 1284–1286 (1996)
- D.H. Hathaway, The solar cycle. *Living Rev. Sol. Phys.* **7**, 1 (2010)
- F. Hill, R. Howe, R. Komm, J. Christensen-Dalsgaard, T.P. Larson, J. Schou, M.J. Thompson, Large-scale zonal flows during the solar minimum – where is cycle 25? *Bull. Am. Astron. Soc.* **43**, 16.10 (2011)
- R. Howard, Polar magnetic fields of the Sun: 1960–1971. *Sol. Phys.* **25**, 5–13 (1972)
- R. Howard, B.J. LaBonte, The Sun is observed to be a torsional oscillator with a period of 11 years. *Astrophys. J. Lett.* **239**, L33–L36 (1980)
- R. Howe, Solar interior rotation and its variation. *Living Rev. Sol. Phys.* **6**, 1 (2009)
- R. Howe, J. Christensen-Dalsgaard, F. Hill, R.W. Komm, R.M. Larsen, J. Schou, M.J. Thompson, J. Toomre, Deeply penetrating banded zonal flows in the solar convection zone. *Astrophys. J. Lett.* **533**, L163–L166 (2000a)
- R. Howe, R. Komm, F. Hill, Variations in solar sub-surface rotation from GONG data 1995–1998. *Sol. Phys.* **192**, 427–435 (2000b)
- R. Howe, F. Hill, R. Komm, J. Christensen-Dalsgaard, T.P. Larson, J. Schou, M.J. Thompson, R. Ulrich, The torsional oscillation and the new solar cycle, in *GONG–SoHO 24: A New Era of Seismology of the Sun and Solar-Like Stars*. Journal of Physics: Conference Series, vol. 271 (IOP, Bristol, 2011), Issue 1, id. 012074
- R. Howe, J. Christensen-Dalsgaard, F. Hill, R. Komm, T.P. Larson, M. Rempel, J. Schou, M.J. Thompson, The high-latitude branch of the solar torsional oscillation in the rising phase of cycle 24. *Astrophys. J. Lett.* **767**, L20 (2013), 4 pp.
- A.J. Kinder, Edward Walter Maunder FRAS (1851–1928): his life and times. *J. Br. Astron. Assoc.* **118**, 21–42 (2008)
- R.W. Komm, R.F. Howard, J.W. Harvey, Torsional oscillation patterns in photospheric magnetic features. *Sol. Phys.* **143**, 19–39 (1993)
- R. Komm, R. Howe, I. González Hernández, F. Hill, Solar-cycle variation of subsurface zonal flow. *Sol. Phys.* **289**, 3435–3455 (2014)
- D.F. Kong, Z.N. Qu, Q.L. Guo, Revisiting the question: does high-latitude solar activity lead low-latitude solar activity in time phase? *Astron. J.* **147**, 97 (2014), 7 pp.
- N.A. Krivova, S.K. Solanki, The 1.3-year and 156-day periodicities in sunspot data: wavelet analysis suggests a common origin. *Astron. Astrophys.* **394**, 701–706 (2002)
- M. Küker, R. Arlt, R. Rüdiger, The Maunder minimum as due to magnetic Δ -quenching. *Astron. Astrophys.* **343**, 977–982 (1999)
- B.J. LaBonte, R. Howard, Torsional waves on the sun and the activity cycle. *Sol. Phys.* **75**, 161–178 (1982)
- N. Labrosse, S. Dalla, S. Marshall, Automatic detection of limb prominences in 304 Å EUV images. *Sol. Phys.* **262**, 449–460 (2010)
- J.L. Leroy, On the orientation of magnetic fields in quiescent prominences. *Astron. Astrophys.* **64**, 247–252 (1978)
- J.-L. Leroy, J.-C. Noens, Does the solar activity cycle extend over more than an 11-year period? *Astron. Astrophys.* **120**, L1–L2 (1983)
- K.J. Li, Latitude migration of solar filaments. *Mon. Not. R. Astron. Soc.* **405**, 1040–1046 (2010)

- K.J. Li, Q.X. Li, P.X. Gao, X.J. Shi, Cyclic behavior of solar full-disk activity. *J. Geophys. Res.* **113**, A11108 (2008)
- W. Livingston, T.L. Duvall Jr., Solar rotation, 1966–1978. *Sol. Phys.* **61**, 219–231 (1979)
- W.J.S. Lockyer, On the relationship between solar prominences and the forms of the corona. *Mon. Not. R. Astron. Soc.* **91**, 797–809 (1931)
- N. Lockyer, W.J.S. Lockyer, Solar prominence and spot circulation, 1872–1901. *Proc. R. Soc. Lond.* **71**, 446–452 (1902)
- D.H. Mackay, C.R. DeVore, S.K. Antiochos, Global-scale consequences of magnetic-helicity injection and condensation on the Sun. *Astrophys. J.* **784**, 164 (2014), 15 pp.
- V.I. Makarov, K.R. Sivaraman, Evolution of latitude zonal structure of the large-scale magnetic field in solar cycles. *Sol. Phys.* **119**, 35–44 (1989a)
- V.I. Makarov, K.R. Sivaraman, New results concerning the global solar cycle. *Sol. Phys.* **123**, 367–380 (1989b)
- S.F. Martin, Conditions for the formation and maintenance of filaments (Invited review). *Sol. Phys.* **182**, 107–137 (1998)
- S.F. Martin, K.H. Harvey, Ephemeral active regions during solar minimum. *Sol. Phys.* **64**, 93–108 (1979)
- E.W. Maunder, Note on the distribution of sun-spots in heliographic latitude, 1874–1902. *Mon. Not. R. Astron. Soc.* **64**, 747–761 (1904)
- A.R. Maunder, Letter to Stephan Ionides 21 May 1940 (1940)
- P.S. McIntosh, Solar interior processes suggested by large-scale surface patterns, in *The Solar Cycle*, ed. by K.L. Harvey. ASP Conference Series, vol. 27 (ASP, San Francisco, 1992), pp. 14–34
- H.W. Newton, *The Face of the Sun* (Penguin, Baltimore, 1958), p. 116
- W.D. Pesnell, Solar cycle predictions. *Sol. Phys.* **281**, 507–532 (2012)
- G.J.D. Petrie, K. Petrovay, K. Schatten, Solar polar fields and the 22-year activity cycle: observations and models. *Space Sci. Rev.* (2014). doi:10.1007/s11214-014-0064-4
- V.V. Pipin, The Gleissberg cycle by a nonlinear $\alpha\Lambda$ dynamo. *Astron. Astrophys.* **346**, 295–302 (1999)
- M. Rempel, Flux-transport dynamos with Lorentz force feedback on differential rotation and meridional flow: saturation mechanism and torsional oscillations. *Astrophys. J.* **647**, 662–675 (2006)
- M. Rempel, High-latitude solar torsional oscillations during phases of changing magnetic cycle amplitude. *Astrophys. J. Lett.* **750**, L8 (2012), 4 pp.
- A. Riccò, Risultati delle osservazioni dell protuberanze solari nel periodo undecennale dell'attività solare dal 1880 al 1890. *Mem. Soc. degli Spettro. Ital.* **20**, 135–139 (1892)
- E. Robbrecht, Y.-M. Wang, N.R. Sheeley Jr., N.B. Rich, On the “extended” solar cycle in coronal emission. *Astrophys. J.* **716**, 693–700 (2010)
- D.M. Rust, Magnetic fields in quiescent solar prominences. I. Observations. *Astrophys. J.* **150**, 313–326 (1967)
- M. Rybanský, V. Rušin, M. Minarovjech, L. Klocok, E.W. Cliver, Reexamination of the coronal index of solar activity. *J. Geophys. Res.* **110**, A08106 (2005), 9 pp.
- K.H. Schatten, P.H. Scherrer, L. Svalgaard, J.M. Wilcox, Using dynamo theory to predict the sunspot number during solar cycle 21. *Geophys. Res. Lett.* **5**, 411–414 (1978)
- P.H. Scherrer, R.S. Bogart, R.I. Bush, J.T. Hoeksema, A.G. Kosovichev, J. Schou, W. Rosenberg, L. Springer et al., The solar oscillations investigation – Michelson Doppler Imager. *Sol. Phys.* **162**, 129–188 (1995)
- J. Schou, Migration of zonal flows detected using Michelson Doppler Imager f -mode frequency splittings. *Astrophys. J. Lett.* **523**, L181–L184 (1999)
- J. Schou, H.M. Antia, S. Basu, R.S. Bogart, R.I. Bush, S.M. Chitre, J. Christensen-Dalsgaard, M.P. Di Mauro et al., Helioseismic studies of differential rotation in the solar envelope by the solar oscillations investigation using the Michelson Doppler Imager. *Astrophys. J.* **505**, 390–417 (1998)
- J. Schou, P.H. Scherrer, R.I. Bush, R. Wachter, S. Couvidat, M.C. Rabello-Soares, R.S. Bogart, J.T. Hoeksema et al., Design and ground calibration of the Helioseismic and Magnetic Imager (HMI) instrument on the Solar Dynamics Observatory (SDO). *Sol. Phys.* **275**, 229–259 (2012)
- M.A. Schuh, J.M. Banda, P.N. Bernasconi, R.A. Angryk, P.C.H. Martens, A comparative evaluation of automated solar filament detection. *Sol. Phys.* **289**, 2503–2524 (2014)
- M. Schüssler, The solar torsional oscillation and dynamo models of the solar cycle. *Astron. Astrophys.* **94**, L17–L18 (1981)
- S.H. Schwabe, Sonnen-Beobachtungen in Jahre 1843. *Astron. Nachr.* **21**, 233–236 (1844)
- H.J. Smith, E.v.P. Smith, *Solar Flares* (Macmillan, New York, 1963), p. 30
- H.B. Snodgrass, Solar torsional oscillations—a net pattern with wavenumber 2 as artifact. *Astrophys. J.* **291**, 339–343 (1985)
- H.B. Snodgrass, Synoptic observations of large scale velocity patterns on the Sun, in *The Solar Cycle*, ed. by K.L. Harvey. ASP Conference Series, vol. 27 (ASP, San Francisco, 1992), pp. 205–240

- G. Spörer, Beobachtungen der Sonnenflecken vom Januar 1874 bis December 1879. *Publ. Astrophys. Obs. Potsdam* **2**(5), 1–81 (1880)
- H.C. Spruit, Origin of the torsional oscillation pattern of solar rotation. *Sol. Phys.* **213**, 1–21 (2003)
- L. Svalgaard, Y. Kamide, Asymmetric solar polar field reversals. *Astrophys. J.* **763**, 23 (2013), 6 pp.
- L. Svalgaard, E.W. Cliver, Y. Kamide, Sunspot cycle 24: smallest cycle in 100 years? *Geophys. Res. Lett.* **32**, L01104 (2005)
- S.J. Tappin, R.C. Altrock, The extended solar cycle tracked high into the corona. *Sol. Phys.* **282**, 249–261 (2013)
- M.J. Thompson, J. Toomre, E. Anderson, H.M. Antia, G. Berthomieu, D. Burtonclay, S.M. Chitre, J. Christensen-Dalsgaard et al., Differential rotation and dynamics of the solar interior. *Science* **272**, 1300–1305 (1996)
- J. Toomre, J. Christensen-Dalsgaard, R. Howe, R.M. Larsen, J. Schou, M.J. Thompson, Time variability of rotation in solar convection zone from SOI-MDI. *Sol. Phys.* **192**, 437–448 (2000)
- K. Topka, R. Moore, B.J. Labonte, R. Howard, Evidence for a poleward meridional flow on the Sun. *Sol. Phys.* **79**, 231–245 (1982)
- R.K. Ulrich, Very long lived wave patterns detected in the solar surface velocity signal. *Astrophys. J.* **560**, 466–475 (2001)
- R.K. Ulrich, T. Tran, The global solar magnetic field—identification of traveling, long-lived ripples. *Astrophys. J.* **768**, 189 (2013), 12 pp.
- S.V. Vorontsov, J. Christensen-Dalsgaard, J. Schou, V.N. Strakhov, M.J. Thompson, Helioseismic measurement of solar torsional oscillations. *Science* **296**, 101–103 (2002)
- M. Waldmeier, Zirkulation und Magnetfeld der solaren Polarzone. *Z. Astrophys.* **49**, 176–185 (1960)
- M. Waldmeier, A secondary polar zone of solar prominences. *Sol. Phys.* **28**, 389–398 (1973)
- Y.-M. Wang, N.R. Sheeley Jr., S.H. Hawley, J.R. Kraemer, G.E. Brueckner, R.A. Howard, C.M. Korendyke, D.J. Michels et al., The green line corona and its relation to the photospheric magnetic field. *Astrophys. J.* **485**, 419–429 (1997)
- D.F. Webb, CMEs and prominences and their evolution over the solar cycle, in *New Perspectives on Solar Prominences, IAU Colloquium 167*, ed. by D. Webb, D. Rust, B. Schmieder. ASP Conference Series, vol. 150 (ASP, San Francisco, 1997), pp. 463–474
- P.R. Wilson, R.C. Altrock, K.L. Harvey, S.F. Martin, H.B. Snodgrass, The extended solar activity cycle. *Nature* **333**, 748–750 (1988)
- H. Yoshimura, Solar cycle Lorentz force waves and the torsional oscillations of the Sun. *Astrophys. J.* **247**, 1102–1112 (1981)
- C.A. Young, in *The Sun*, 4th edn. (Appleton, New York, 1897), pp. 157
- P. Zeeman, On the influence of magnetism on the nature of the light emitted by a substance. *Astrophys. J.* **5**, 332–347 (1897)